© 2002 The Chemical Society of Japan

Preparation and Properties of Tin(IV) Complexes with the Sulfur-Rich Dithiolate C_3S_5 and $C_8H_4S_8$ Ligands and Their Oxidation

Tenpei Akasaka, Motohiro Nakano, Hatsue Tamura, and Gen-etsu Matsubayashi*

Department of Applied Chemistry & Frontier Research Center, Graduate School of Engineering, Osaka University, 1-16, Machikaneyama, Toyonaka, Osaka 560-0043

(Received June 13, 2002)

$[NMe_4]_2[Sn(C_3S_5)_3]$, $[NBu^n_4]_2[Sn(C_3S_5)_3]$, $[NBu^n_4]_2[Sn(C_8H_4S_8)_3]$, $[NEt_4][Sn(Bu^n)(C_8H_4S_8)_2]$ and $[NBu^n_4][Sn(Ph)(C_8H_4S_8)_2]$ [$C_3S_5^{2-}$ = 4,5-disulfanyl-1,3-dithiole-2-thionate(2−) ; $C_8H_4S_8^{2-}$ = 2-{(4,5-ethylenedithio)-1,3-dithiole-2-ylidene}-1,3-dithiole-4,5-ditholate(2−)] were prepared by reactions of $Na_2[C_3S_5]$ or $Na_2[C_8H_4S_8]$ with $SnCl_4 \cdot 5H_2O$, $Sn(Bu^n)Cl_3$ and $Sn(Ph)Cl_3$ in EtOH. $[NBu^n_4]_2[Sn(C_8H_4S_8)_3]$ was oxidized by iodine or TCNQ in DMF/CH_2Cl_2 to give $[Sn(C_8H_4S_8)_3]$, which exhibited an electrical conductivity of 3.2×10^{-2} S cm^{-1} (compacted pellet at room temperature). $[NBu^n_4]_2[Sn(C_3S_5)_3]$, $[NEt_4][Sn(Bu^n)(C_8H_4S_8)_2]$ and $[NBu^n_4][Sn(Ph)(C_8H_4S_8)_2]$ were oxidized by iodine or TCNQ in acetone or in DMF to afford $(C_3S_5)_2$ and $(C_8H_4S_8)_n$. Crystal structures of $[NMe_4]_2[Sn(C_3S_5)_3]$, $[NBu^n_4]_2[Sn(C_3S_5)_3]$, $[NBu^n_4][Sn(Ph)(C_8H_4S_8)_2]$ and $(C_3S_5)_2$ were determined by X-ray crystallography.

Oxidized, planar metal complexes with the 4,5-disulfanyl-1,3-dithiole-2-thionate(2−) ligand, $[M(C_3S_5)_2]^{n-}$ (M = Ni(II), Pd(II), Pt(II) and Au(III); $n < 1$) species, are known as good electrical conductors[1–4] and some planar Ni(II), Pt(II) and Au(III)-complexes with the $C_8H_4S_8^{2-}$ ligand [2-{(4,5-ethylenedithio)-1,3-dithiole-2-ylidene}-1,3-dithiole-4,5-ditholate(2−)] are also oxidized to become electrical conductors with high electrical conductivities.[5–8] Non-planar, bulky metal complexes with these sulfur-rich dithiolate ligands attract much interest because of their unique molecular interactions caused by new molecular packings in the solid state. Partially oxidized $[M(C_3S_5)_3]^{m-}$ (M = Mo(IV), W(IV)[9] and Re(IV)[10]; $m < 1$) and $[Re_2(C_3S_5)_5]^{m-}$ ($m < 1$) complexes[11] exhibited also high electrical conductivities owing to the formation of electron-conduction pathways through S···S non-bonded contacts in the solid state. Bulky penta- and hexa-coordinate metal complexes having the $C_8H_4S_8$ ligand as a further extended π-electron system are also expected to become good electrical conductors due to more effective molecular interactions through more S···S contacts. Non-planar $[M(O)(C_8H_4S_8)_2]^{2-}$ [M = V(IV) and Mo(IV)],[12] $[Co(\eta^5\text{-}C_5H_5)(C_8H_4S_8)]$[13] and $[M(\eta^5\text{-}C_5H_5)(C_8H_4S_8)_2]^-$ [M = Ti(IV) and Zr(IV)] complexes[14–16] were oxidized to yield the complexes with high electrical conductivities. Several non-planar organotin(IV)-complexes with the C_3S_5 ligand were prepared and some crystal structures were clarified.[17–23] However, their oxidation processes and properties of oxidized species have not been studied.

In this work, some penta- and hexa-coordinate $C_8H_4S_8$-tin(IV) and -organotin(IV) complexes with non-planar geometries, as well as $[Sn(C_3S_5)_3]^{2-}$ complexes, have been prepared and their oxidation has been performed. Electrochemical and spectroscopic properties of the complexes are described, as well as electrical conductivities of the oxidized species. X-ray crystal structures of $[NMe_4]_2[Sn(C_3S_5)_3]$, $[NBu^n_4]_2[Sn(C_3S_5)_3]$ and $[NBu^n_4][Sn(Ph)(C_8H_4S_8)_2]$, as well as that of $(C_3S_5)_2$ obtained by the oxidation of the $[Sn(C_3S_5)_3]^{2-}$ complexes, have been also clarified.

Experimental

Preparation. 4,5-Bis(benzoylthio)-1,3-dithiole-2-thione, $C_3S_5(COPh)_2$,[24,25] and 4,5-bis(cyanoethylthio)-1,3-dithiole-[(4,5-ethylenedithio)-1,3-dithiole-2-ylidene], $C_8H_4S_8(CH_2CH_2CN)_2$,[7,26,27] were prepared according to the literature methods. 7,7,8,8-Tetracyano-*p*-quinodimethane (TCNQ) and butyl- and phenyltrichlorotin(IV) were commercially available. All the following reactions were performed under an argon atmosphere.

$[NMe_4]_2[Sn(C_3S_5)_3]$ (1). To a THF (50 cm^3) solution of $C_3S_5(COPh)_2$ (500 mg, 1.2 mmol) was added with vigorous stirring an MeOH (3.9 cm^3) solution containing NMe_4OH (0.97 mg, 2.6 mmol) and the solution was stirred for 15 min. The resulting red brown solids of $[NMe_4]_2[C_3S_5]$ were filtered. To the EtOH (35 cm^3) solution of them was added with stirring an EtOH (5 cm^3) solution of $SnCl_4 \cdot 5H_2O$ (210 mg, 0.60 mmol) and the solution was stirred for 17 h at room temperature. The resulting solids of **1** were filtered, washed with H_2O, EtOH, diethyl ether and *n*-hexane, and dried in vacuo (84% yield). Calcd for $C_{17}H_{24}N_2S_{15}Sn$: C, 23.85; H, 2.83; N, 3.27%. Found: C, 23.63; H, 2.88; N, 3.33%. IR (KBr disk) 897, 948, 1028, 1058, 1067, 1409, 1477 cm^{-1}. Recrystallization from hot MeOH afforded dark red prisms for the X-ray crystallography.

$[NBu^n_4]_2[Sn(C_3S_5)_3]$ (2). It was prepared by a similar reaction in the presence of NBu^n_4Cl (74% yield). Calcd for $C_{41}H_{72}N_2S_{15}Sn$: C, 41.29; H, 6.08; N, 2.35%. Found: C, 41.06; H, 5.91; N, 2.42%. IR (KBr disk) 738, 894, 1036, 1056, 1067, 1145, 1376, 1422, 1439, 1479, 2866, 2956 cm^{-1}. Recrystallization from hot MeOH afforded dark red prisms for the X-ray crystallography.

$[NBu^n_4]_2[Sn(C_8H_4S_8)_3]$ (3). It was prepared as follows. $C_8H_4S_8(CH_2CH_2CN)_2$ (1.7 g, 3.6 mmol) was dissolved with stirring into an EtOH (140 cm^3) solution containing sodium metal (820 mg, 36 mmol) for 1 h under ultrasonic waves. To the resulting red brown solution of $Na_2[C_8H_4S_8]$ was added with stirring an EtOH (20 cm^3) solution of $SnCl_4 \cdot 5H_2O$ (630 mg, 1.8 mmol) and NBu^n_4Cl (1.0 g, 3.6 mmol) and the solution was stirred for 8 h at room temperature. The resulting solids of **3** were collected by filteration, washed with H_2O, EtOH and diethyl ether, and dried in vacuo (90% yield). Calcd for $C_{56}H_{84}N_2S_{24}Sn$: C, 40.19; H, 5.06; N, 1.67%. Found: C, 39.96; H, 4.91; N, 1.77%. IR (KBr disk) 736, 772, 882, 1167, 1286, 1377, 1409, 1477, 2867, 2955 cm^{-1}. ^{1}H NMR ($CDCl_3$) δ 0.96 (24H, t, CH_3), 1.33 (16H, m, CH_2), 1.56 (16H, m, CH_2), 3.06 (16H, t, CH_2), 3.30 (12H, t, CH_2).

$[NEt_4][Sn(Bu^n)(C_8H_4S_8)_2]$ (4). It was prepared similarly by a reaction of $Na_2[C_8H_4S_8]$ with $Sn(Bu^n)Cl_3$ and NEt_4Cl in EtOH as described for **3** (50% yield). Calcd for $C_{28}H_{37}NS_{16}Sn$: C, 33.00; H, 3.66; N, 1.37%. Found: C, 32.93; H, 3.50; N, 1.58%. IR (KBr disk) 771, 887, 917, 998, 1054, 1170, 1284, 1361, 1388, 1407, 1433, 1454, 1477, 1513, 2863, 2911, 2949 cm^{-1}. ^{1}H NMR (acetone-d_6) δ 0.91 (3H, t, CH_3), 1.39 (12H, m, CH_3), 1.40–1.80 (6H, m, CH_2), 3.39 (8H, s, CH_2), 3.50 (8H, q, CH_2).

$[NBu^n_4][Sn(Ph)(C_8H_4S_8)_2]$ (5). It was prepared by a reaction of $Na_2[C_8H_4S_8]$ with $Sn(Ph)Cl_3$ and NBu^n_4Cl in EtOH as described for **3** (60% yield). Calcd for $C_{38}H_{49}NS_{16}Sn$: C, 39.64; H, 4.29; N, 1.22%. Found: C, 39.71; H, 3.90; N, 1.35%. IR (KBr disk) 738, 771, 888, 919, 1024, 1070, 1105, 1151, 1170, 1288, 1375, 1406, 1459, 1476, 2864, 2918, 2952 cm^{-1}. ^{1}H NMR (acetone-d_6) δ 0.97 (12H, t, CH_3), 1.43 (8H, m, CH_2), 1.82 (8H, m, CH_2), 3.39 (8H, s, CH_2), 3.44 (8H, t, CH_2), 7.38 (3H, m, *m*,*p*-C_6H_5), 7.79 (2H, *m*, *o*-C_6H_5, $^2J(^{119}Sn–^1H)$, 88 Hz). Solids of **5** were recrystallized from a THF/EtOH mixture in a refregirator for 2 d to give dark red prisms for the X-ray crystallography.

$[Sn(C_8H_4S_8)_3]$ (6). To a DMF/CH_2Cl_2 (1:1 v/v) mixture solution (20 cm^3) containing **3** (120 mg, 0.072 mmol) was added a DMF/CH_2Cl_2 (1:4 v/v) mixture solution (50 cm^3) having TCNQ (77 mg, 0.38 mmol), followed by stirring for 15 min. The resulting black solids of **6** were collected by filtration, washed with CH_2Cl_2, EtOH, acetone and diethyl ether, and dried in vacuo (56% yield). Calcd for $C_{24}H_{12}S_{24}Sn$: C, 24.25; H, 1.02%. Found: C, 24.33; H, 1.35%. IR (KBr disk) 1300, 1378, 1411, 1462 cm^{-1}.

$[C_8H_4S_8]_n$ (7). A THF (200 cm^3) solution of TCNQ (200 mg, 1.0 mmol) was added to a DMF (120 cm^3) solution of **4** (100 mg, 0.10 mmol) and the solution was stirred for 30 min. at room temperature to afford grey solids of **7**. They were collected by filtration, washed with acetone, and dried in vacuo (68% yield). Calcd for $C_8H_4S_8$: C, 26.95; H, 1.13%. Found: C, 27.17; H, 1.28%. IR (KBr disk) 767, 883, 958, 1118, 1283, 1403, 1461 cm^{-1}. A similar reaction of **5** with TCNQ in a DMF/THF mixture also yielded solids of **7** (45% yield). Calcd for $C_8H_4S_8$: C, 26.95; H, 1.13%. Found: C, 27.31; H, 1.30%.

$[C_8H_4S_8\ I_{0.9}]_n$ (8). To a diethyl ether (40 cm^3) solution containing iodine (170 mg, 0.68 mmol) was added fine powders of **7** (64 mg, 0.18 mmol) and the suspended solution was stirred for 16 h at room temperature. The resulting black solids of **8** were collected by filtration, washed with diethyl ether and acetone, and dried in vacuo (75% yield). Calcd for $C_8H_4S_8I_{0.9}$: C, 26.95; H, 1.13%. Found: C, 27.17; H, 1.28%. IR (KBr disk) 767, 883, 958, 1118, 1283, 1403, 1461 cm^{-1}. The presence of I_3^- and I_5^- ions was confirmed by Raman spectra as described below.

$(C_3S_5)_2$ (9). To an acetone (25 cm^3) solution of **1** (180 mg, 0.15 mmol) was added a THF (150 cm^3) solution of TCNQ (300 mg, 1.5 mmol) and the solution was allowed to stand at room temperature for 3 d to afford dark red needles of **9**. They were collected by filtration, washed with acetone, and dried in vacuo (56% yield). Calcd for C_6S_{10}: C, 18.35%. Found: C, 18.27%. IR (KBr disk) 1054, 1444 cm^{-1}. The structure of **9** was determined by X-ray crystallography, as described below.

Physical Measurements. IR, electronic absorption, ESR,[28] and powder reflectance spectra[29] were recorded as described previously. ^{1}H NMR spectra were recorded at 270 MHz using a JEOL EX-270 spectrometer, the chemical shifts being measured relative to tetramethylsilane as an internal standard in an organic solvent. Raman spectra were measured using a Nipponbunko NR-1800 laser-Raman spectrophotometer. Cyclic voltammograms of the complexes in CH_2Cl_2 or in DMF were measured using $[NBu^n_4][ClO_4]$ as an electrolyte. Electrical resistivities of the complexes were measured at room temperature for compacted pellets by the conventional two-probe method.[29]

X-ray Data Collection. Intensity data were collected on a Rigaku RAXIS-RAPID imaging plate diffractometer for **1** and **5**, a Rigaku AFC-7R diffractometer for **2** and a Rigaku AFC-5R diffractometer for **9**, at the Graduate School of Science, Osaka University, with graphite-monochromated Mo-Kα radiation (λ = 0.71069 Å). Crystal data and details of measurements for complexes **1**, **2** and **5** and compound **9** are summarized in Table 1. For the data collection up to $2\theta = 55°$, two sets of exposures (θ = 0.0°, χ = 45.0° and ω = 130.0° to 190.0°; θ = 180.0°, χ = 45.0° and ω = 0.0° to 160.0°) were measured by scans of 4° and 5° in ω for **1** and for **5**, respectively. The intensity data were processed using the PROCESS-AUTO program package and corrected for Lorentz and polarization effects as well as absorption by the Higashi method[30] (transmission factors, 0.609–0.950 for **1**, and 0.761–0.892 for **5**). Cell constants were obtained by least-squares refinement of 31437 reflections ($3.2° < 2\theta < 54.9°$) for **1** and of 10990 reflections ($4.9° < 2\theta < 55.0°$) for **5**. Intensity data were collected in the ω–2θ scan mode up to $2\theta = 50°$ for **2** and up to 60° for **9**. The intensities of three standard reflections were monitored every 150 reflections for the crystal orientation and stability. No significant decay was observed through the collections. The reflection data were corrected for Lorentz and polarization factors as well as absorption by the North–Phillips method[31] (transmission factors, 0.677–0.905 for **2** and 0.679–0.847 for **9**). Cell constants and orientation matrices were determined by least-squares refinement of the setting angles of 25 reflections in the ranges $23.4° < 2\theta < 24.0°$ for **2** and $23.8° < 2\theta < 24.9°$ for **9**.

Crystal Structure Determinations and Refinements. The structures of **1**, **2** and **5** were solved by the direct methods using SHELXS86[32] or SIR92[33] and refined on F^2 by the full-matrix least-squares technique with SHELXL97.[34] All the non-hydrogen atoms except for the phenyl group atoms of **5** and disordered atoms in the tetraalkylammonium cations were refined anisotropically. Since the tetramethylammonium cations of **1** and one of four butyl groups of the tetrabutylammonium cation of **5** adopted disordered structures, the positional parameters of hydrogen atoms were not determined. The positions of other hydrogen atoms were geometrically calculated and refined with isotropic thermal parameters riding on those of the parant atoms. The structure of **1** was refined using the instruction TWIN to give Flack parameter to be 0.58(4), which indicates the presence of a twin by inversion center. The assignment of three peaks (up to 2.2 e Å^{-3}) on a difference Fourier map for **5** was unsuccessful. The structure of **9**

Table 1. Crystallographic Data for $[NMe_4]_2[Sn(C_3S_5)_3]$ (**1**), $[NBu^n_4]_2[Sn(C_3S_5)_3]$ (**2**), $[NBu^n_4][Sn(Ph)(C_8H_4S_8)_2]$ (**5**) and $(C_3S_5)_2$ (**9**)

	1	**2**	**5**	**9**
Empirical formula	$C_{17}H_{24}N_2S_{15}Sn$	$C_{41}H_{72}N_2S_{15}Sn$	$C_{38}H_{49}NS_{16}Sn$	C_6S_{10}
Molecular weight	855.98	1192.77	1151.58	392.66
Crystal system	Orthorhombic	Monoclinic	Triclinic	Monoclinic
Space group	$P2_12_12_1$	$C2/c$	$P\bar{1}$	$P2_1/a$
a/Å	15.2757(5)	19.849(3)	13.1800(7)	7.773(2)
b/Å	22.7319(6)	14.243(2)	17.2992(8)	10.591(2)
c/Å	9.6723(2)	21.635(2)	13.0153(8)	8.186(2)
α/°	90	90	108.848(3)	90
β/°	90	107.017	107.647(2)	105.21(2)
γ/°	90	90	96.752(2)	90
V/Å^3	3348.7(2)	5848(1)	2598.7(3)	650.3(2)
Z	4	4	2	2
T/K	296	296	296	296
μ/mm^{-1}	1.71	1.00	1.14	1.66
Reflection collected	31434	5310	24942	2132
Independent reflections	4306	5149	11794	1906
Observed reflections ($I > 2\sigma(I)$)	3191	2518	7333	1241
R, wR ($I > 2\sigma(I)$)	0.041, 0.102	0.055, 0.158	0.066, 0.202	0.033, 0.038
R, wR (all data)	0.055, 0.108	0.143, 0.203	0.108, 0.233	

was solved by the direct method with SIR92 and refined on F anisotropically using teXsan package.[35]

Calculations were performed on an SGI-O2 workstation at the Graduate School of Science, Osaka University. Atomic scattering factors were taken from the usual sources.[36] Figures 1–6 were drawn with a local version of ORTEP II.[37]

Crystallographic data (excluding structure factors) have been deposited at the CCDC, 12 Union Road, Cambridge CB2 1EZ, UK and copies can be obtained on request, free of charge, by quoting the publication citation and deposition number CCDC 171452–171455. The data are also deposited as Document No. 75057 at the Office of the Editor of Bull. Chem. Soc. Jpn.

Results and Discussion

Crystal Structures of 1 and 2. Perspective views of the anion moieties of **1** and **2** are illustrated in Fig. 1, together with the atom numbering scheme. Bond distances and angles relevant to the tin coordination spheres of these complexes are listed in Table 2. The structures of the anions of both the complexes show three C_3S_5 ligands coordinated to the tin atom. Interligand transoid S–Sn–S angles are 170.8° and 171.5° (aver-

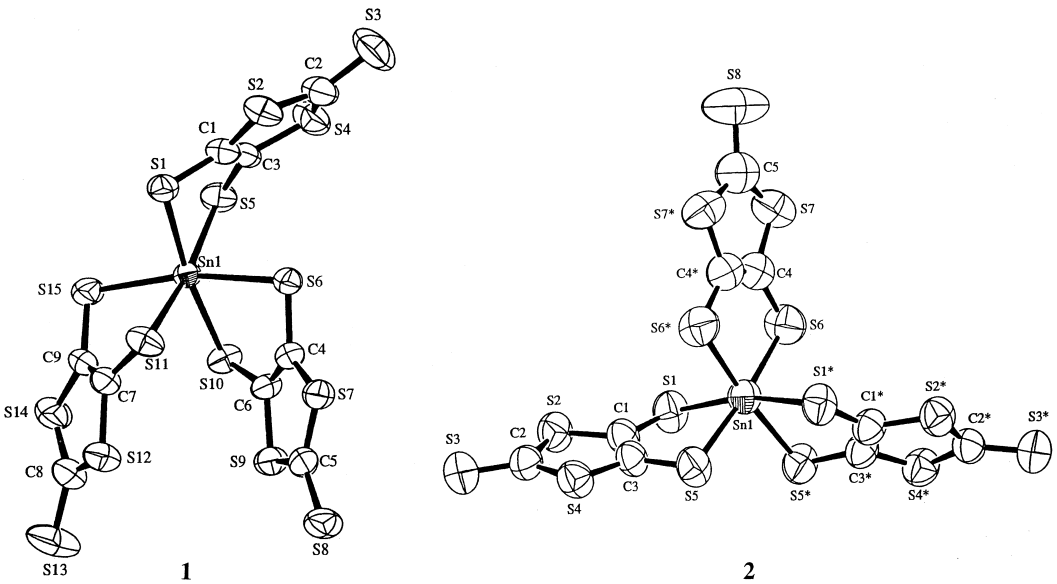

Fig. 1. Geometries of the anion moieties of $[NMe_4]_2[Sn(C_3S_5)_3]$ (**1**) and $[NBu^n_4]_2[Sn(C_3S_5)_3]$ (**2**) with atom numbering scheme. Sn, C(5) and S(8) atoms are on the C_2 axis for **2**.

Table 2. Selected Bond Lengths (Å) and Angles (°) for the Anion Moieties of $[NMe_4]_2[Sn(C_3S_5)_3]$ (**1**) and $[NBu^n{}_4]_2[Sn(C_3S_5)_3]$ (**2**)

	1		**2***
Sn–S(1)	2.534(2)		2.574(2)
Sn–S(5)	2.564(2)		2.525(2)
Sn–S(6)	2.580(2)		2.512(2)
Sn–S(10)	2.558(2)		
Sn–S(11)	2.552(2)		
Sn–S(15)	2.561(2)		
S(1)–Sn–S(10)	172.83(7)	S(1)–Sn–S(6*)	167.28(11)
S(5)–Sn–S(11)	171.43(7)	S(5)–Sn–S(6)	173.58(8)
S(6)–Sn–S(15)	168.22(6)		
S(1)–Sn–S(5)	81.48(7)	S(1)–Sn–S(5)	83.54(7)
S(6)–Sn–S(10)	82.59(6)	S(6)–Sn–S(6*)	87.20(11)
S(11)–Sn–S(15)	81.94(8)		

*Sn, C(5) and S(8) atoms are on the C_2 axis.

age), for **1** and **2**, respectively, with the limiting angles of 136° and 180° for a trigonal prism and a perfect octahedron. They are different from the geometries rather close to the trigonal prism for $[NBu^n{}_4]_2[M(C_3S_5)_3]$ (transoid S–M–S angle, M = Mo(IV), 146.5° and M = W(IV), 147.2°).[9] The average Sn-S distances for these complexes (**1**, average 2.558 and **2**; 2.536 Å) are close to those for some C_3S_5-tin(IV) anion complexes: $[SnI_2(C_3S_5)_2]^{2-}$ (average 2.545 Å),[19] $[Sn(Me_2)Cl(C_3S_5)]^-$ [2.451(3), 2.662(3) Å],[17] $[Sn(Bu^n)(C_3S_5)_2]^-$ [2.461(5), 2.549(4) Å], $[Sn(Ph)(C_3S_5)_2]^-$ [2.438(4), 2.523(4) Å],[18] and $[Sn(CH_2CH_2CO_2Me)(C_3S_5)_2]^-$ complexes [average 2.511 Å].[21] They are rather longer than those for $[M(C_3S_5)_3]^{2-}$ complexes [M = Mo(IV) (average 2.404 Å) and W(IV) (average 2.394 Å).[9] Didentate dithiolene ligands, S(1)–S(5) and C(1)–C(3), S(6)–S(10) and C(4)–C(6), and S(11)–S(15) and C(7)–C(9), are almost planar with displacements from the least planes of ±0.05 and ±0.01 Å (average) for **1** and **2**, respectively, while the C_3S_5 ligands are appreciably bent on coordinating sulfur atoms: the dihedral angles between the SnS_2 and C_2S_2 planes are 130° and 151° (average) for **1** and **2**, respectively. These findings are similar to the appreciable deviations of the metal atom from the C_3S_5 plane observed for [*N*-methylpyridinium]$_2$[Cu$(C_3S_5)_2$][38] and $[Fe(\eta^5\text{-}C_5Me_5)_2][W(C_3S_5)_3]$.[9]

Although the crystal structure of **2** consists of discrete anions and cations without any significant close atom-atom contacts among them, some S···S non-bonded contacts (< 3.7 Å) among the anions are observed in the crystal structure of **1** (Fig. 2): S(1)–S(7′) [3.553(3) Å], S(2)···S(8′) [3.550(4) Å], S(4)···S(8′) [3.616(4) Å] and S(11)···S(13*) [3.674(5) Å]. Such molecular contact occurs owing to the presence of the small counter cations, resulting in appreciable deviation of the C_3S_5-Sn moieties from the plane in the crystal phase.

Crystal Structure of 5. Figure 3 shows the molecular structure of the anion of **5** together with the atom numbering scheme. Bond distances and angles relevant to the tin coordination sphere of this complex are listed in Table 3. The pentacoordinate anion moiety has a distorted trigonal bipyramid geometry with S(1), S(9) and C(17) atoms in the equatorial positions and S(8) and S(16) atoms in the axial ones; Sn–S(8) and

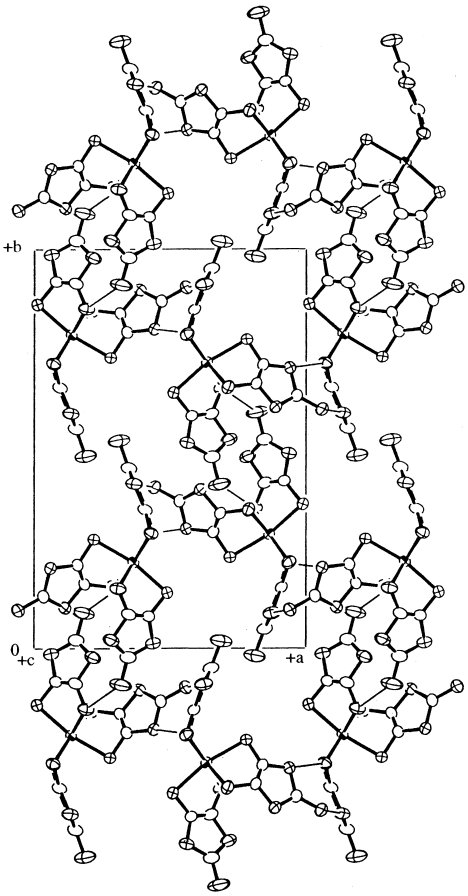

Fig. 2. Packing diagram of the anion moieties of $[NMe_4]_2[Sn(C_3S_5)_3]$ (**1**). Fine lines show non-bonded S···S contacts (< 3.7 Å).

Sn–S(16) bonds are longer than Sn–S(1) and Sn–S(9) ones, and the S(8)–Sn–S(16) angle is 161.57(8)°. This is in contrast to the geometries between square-pyramid and trigonal bipyramid of the $[Sn(R)(C_3S_5)_2]^-$ complexes (R = Bu^n and Ph;[18] $CH_2CH_2CO_2Me$[21]). The Sn–S(axial) distances [2.523(2), 2.571(2) Å] are somewhat longer than the Sn–S(equatorial) ones [2.462(2), 2.471(2) Å]. This is similar to the cases of C_3S_5-organotin(IV) complexes with a trigonal bipyramidal geometry: $[Sn(Me_2)Cl(C_3S_5)]^-$ [Sn–S(ax), 2.662(3); Sn–S(eq), 2.451(3) Å],[17] and $[Sn(Ph_2)(NCS)(C_3S_5)]^-$ complexes [Sn–S(ax), 2.5917(10); Sn–S(eq), 2.4399(10) Å].[22] S(2), S(3), S(6), S(7), C(2) and C(3) atoms are almost coplanar (± 0.04 Å). The planes formed by S(1), S(2), S(7), S(8), C(1) and C(8) (±0.02 Å) and by S(3), S(4), S(5), S(6), C(4) and C(7) (±0.03 Å) make angles of 4.6° and 18.5°, respectively, with the central tetrathiafulvalene skeleton. This is similar to the other $C_8H_4S_8$ moiety: the central tetrathiafulvalene skeleton (±0.01 Å) makes angles of 22.2° and 14.4° with the side C_2S_4 planes. These tub forms are similar to those of $C_8H_4S_8(CH_2CH_2CN)_2$[7] and $[Ti(\eta^5\text{-}C_5Me_5)_2(C_8H_4S_8)]$.[15]

The anion moieties of **5** form a dimeric unit with some non-bonded S···S contacts [S(4)–S(9′), 3.609(2); S(11)–S(14′), 3.602(2) Å] in the crystals. Among the dimers there are also some non bonded S···S contacts (< 3.7 Å), forming a double-chain interaction along the *b* axis (in Fig. 4).

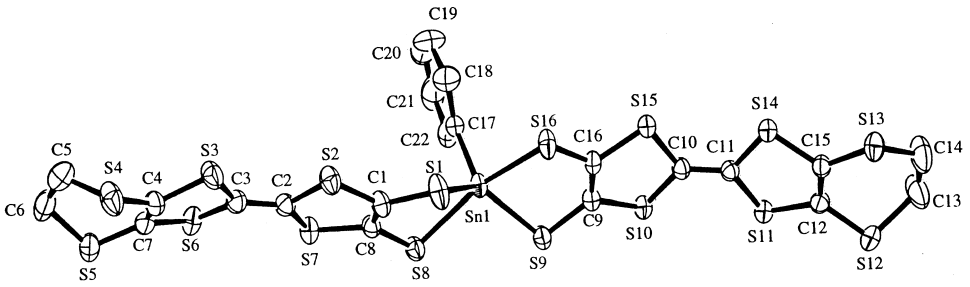

Fig. 3. Geometry of the anion moiety of $[NBu^n_4][Sn(Ph)(C_8H_4S_8)_2]$ (**5**) with atom numbering scheme.

Table 3. Selected Bond Lengths (Å) Angles (°) for the Anion Moiety of $[NBu^n_4][Sn(Ph)(C_8H_4S_8)_2]$ (**5**)

Sn–S(1)	2.4623(18)	Sn–S(8)	2.5705(17)
Sn–S(9)	2.4706(17)	Sn–S(16)	2.5229(18)
Sn–C(17)	2.129(6)	S(1)–C(1)	1.738(7)
S(2)–C(1)	1.776(7)	S(2)–C(2)	1.749(7)
S(3)–C(3)	1.747(7)	S(3)–C(4)	1.751(7)
S(4)–C(4)	1.740(7)	S(4)–C(5)	1.763(14)
S(5)–C(6)	1.812(10)	S(5)–C(7)	1.730(8)
S(6)–C(3)	1.757(8)	S(6)–C(7)	1.765(7)
S(7)–C(2)	1.763(7)	S(7)–C(8)	1.752(6)
S(8)–C(8)	1.741(6)	S(9)–C(9)	1.767(6)
S(10)–C(9)	1.770(6)	S(10)–C(10)	1.766(6)
S(11)–C(11)	1.754(6)	S(11)–C(12)	1.755(7)
S(12)–C(12)	1.744(7)	S(12)–C(13)	1.779(10)
S(13)–C(14)	1.794(10)	S(13)–C(15)	1.750(7)
S(14)–C(11)	1.757(7)	S(14)–C(15)	1.749(6)
S(15)–C(10)	1.761(6)	S(15)–C(16)	1.784(6)
S(16)–C(16)	1.736(6)	C(1)–C(8)	1.344(9)
C(2)–C(3)	1.350(9)	C(4)–C(7)	1.330(11)
C(5)–C(6)	1.511(16)	C(9)–C(16)	1.323(9)
C(10)–C(11)	1.342(8)	C(12)–C(15)	1.339(10)
C(13)–C(14)	1.377(14)		
S(1)–Sn–S(8)	84.20(6)	S(1)–Sn–S(9)	130.75(9)
S(1)–Sn–S(16)	85.29(6)	S(8)–Sn–S(9)	88.60(6)
S(8)–Sn–S(16)	161.57(8)	S(9)–Sn–S(16)	86.84(6)
S(1)–Sn–C(17)	115.42(18)	S(8)–Sn–C(17)	96.98(18)
S(9)–Sn–C(17)	113.80(17)	S(16)–Sn–C(17)	101.20(18)

Crystal Structure of 9. Figure 5 shows the molecular geometry of **9** together with the atom numbering scheme; the crystal structure is illustrated in Fig. 6. The geometry of the dimerized form of C_3S_5 moieties is essentially the same as that of C_6S_{10}·0.5CS_2 previously reported.[39] C–C and S–S bond distances of the C_3S_5 moieties are close to those for C_6S_{12}[40] and C_3S_5-metal complexes reported previously.[9,10,38,41] The S–S distance [2.082(1) Å] is close to those of C_6S_{12} (2.068 Å, average)[40] and the Fe(II) complex with the S–S coupled, C_3S_5-C_3S_5 ligand [2.078(2) Å].[42] The crystal structure consists of many S···S non-bonded contacts (< 3.7 Å), forming a three-dimensional interaction: S(1)···S(3′), 3.215(2); S(3)···S(3′), 3.390(2); S(4)···S(4′), 3.694(2); S(2)···S(3′), 3.467(1); S(4)···S(5′), 3.655(2) Å.

Electrochemical Properties of 1–5. Cyclic voltammograms of **1** and **3** in CH_2Cl_2 and **5** in DMF are shown in Fig. 7. Complex **1** exhibits an irreversible wave with oxidation peak potentials at +0.24 and +0.48 V (vs Ag/Ag^+). A cyclic voltammogram of **2** in acetone has also shown irreversible waves having oxidation peak potentials at +0.27 and +0.48 V (vs Ag/Ag^+). Unstable oxidized species $[Sn(C_3S_5)_3]^{n-}$ (n = 1 and 0) are likely to lead to the cleavage of the Sn–S bond to afford $(C_3S_5)_2$, as described below. On the other hand, **3** shows an irreversible wave with oxidation potentials at −0.20 and + 0.11 V, which correspond to the oxidation processes of $[Sn(C_8H_4S_8)_3]^{2-}/[Sn(C_8H_4S_8)_3]^-$ and $[Sn(C_8H_4S_8)_3]^-/[Sn(C_8H_4S_8)_3]^0$, respectively. This complex shows a further oxidation peak at +0.60 V. These first oxidation peak potentials of **3**

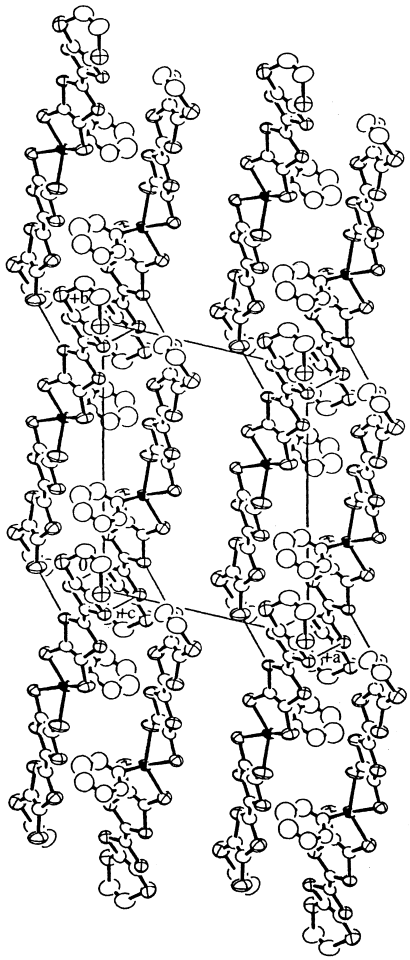

Fig. 4. Packing diagram of the anion moieties of $[NBu^n_4][Sn(Ph)(C_8H_4S_8)_2]$ (**5**). Fine lines show non-bonded S···S contacts (< 3.7 Å).

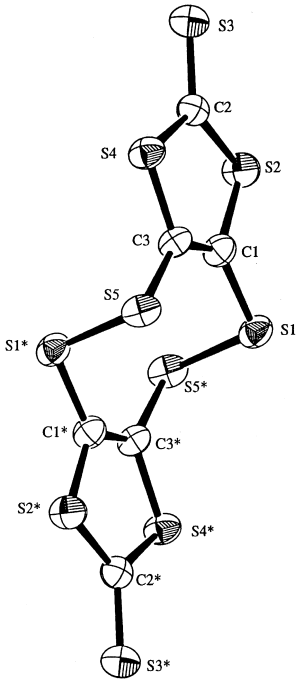

Fig. 5. Molecular structure of $(C_3S_5)_2$ (**9**) with atom numbering scheme.

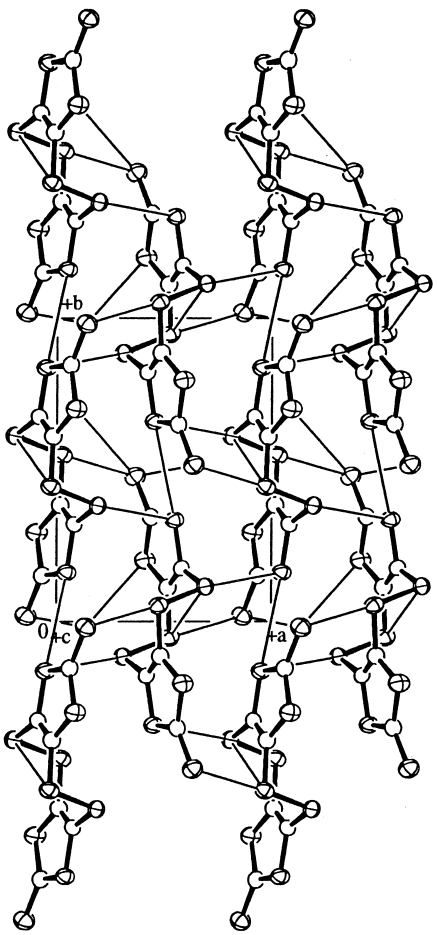

Fig. 6. Crystal structure of $(C_3S_5)_2$ (**9**). Fine lines show nonbonded S···S contacts (< 3.7 Å).

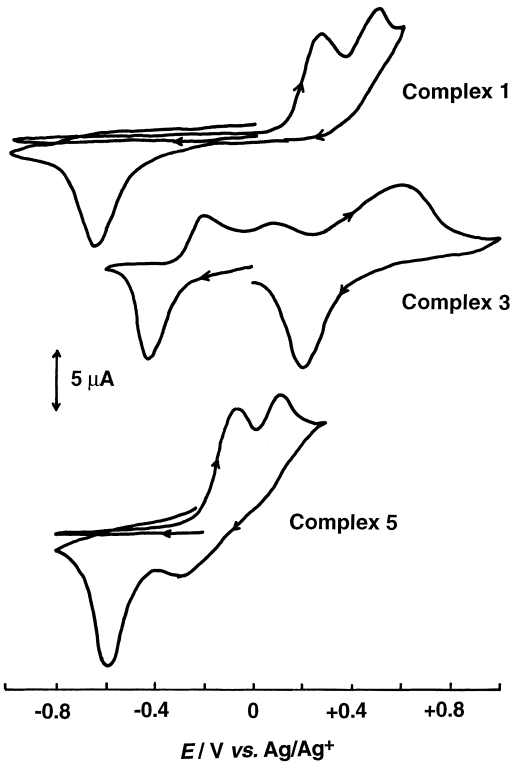

Fig. 7. Cyclic voltammograms of $[NMe_4]_2[Sn(C_3S_5)_3]$ (**1**) and $[NBu^n_4]_2[Sn(C_8H_4S_8)_3]$ (**3**) (1.0×10^{-3} mol dm^{-3}) in CH_2Cl_2 and of $[NBu^n_4][Sn(Ph)(C_8H_4S_8)_2]$ (**5**) (1.0×10^{-3} mol dm^{-3}) in DMF. Supporting electrolyte: 0.1 mol dm^{-3} $[NBu^n_4][ClO_4]$. Sweep rate 0.2 V s^{-1}.

are low compared with those of the corresponding C_3S_5 complexes **1** and **2**, which are the same for those of other $C_8H_4S_8$- and C_3S_5-metal complexes.[7,12,13,15] Complex **5** exhibits an irreversible wave having oxidation peak potentials at -0.09 and $+0.08$ V in DMF. A cyclic voltammogram of **4** has also shown irreversible oxidation peak potentials at -0.13 and $+0.09$ V. Thus, the oxidation of **4** and **5** seems to afford compounds caused by the Sn–S bond cleavage due to the unstability of the oxidized species as described below.

Oxidation of 1–5. A reaction of **1** or **2** with iodine in CH_2Cl_2 has afforded insoluble solids having the composition of $(C_3S_5)_n$. Oxidation of **1** by TCNQ in THF has afforded crystals of C_6S_{10} (**9**). Unstable oxidized species of **1** and **2** quickly cause the Sn–S bond cleavage leading to the combination of the C_3S_5 moieties, as reported for the oxidation of the $[Zn(C_3S_5)_2]^{2-}$ complex.[43] $(C_3S_5)_n$ and **9** have not been further oxidized by excess amounts of iodine and bromine.

Figure 8 shows electronic absorption spectra of **3** in DMF in the presence of various amounts of iodine as an oxidant. The spectral change with isosbestic points indicates the oxidation process corresponding to the electrochemical oxidation. Increasing the amount of iodine, the band at 490 nm due to the π–π^* transition of the $C_8H_4S_8$ ligand diminishes in intensity and shifts to a higher energy; concomitantly the band due to the oxidized species occurs at 850 nm. This band is ascribed to the metal-to-dithiolate ligand charge transfer (CT) transition, since the oxidation occurs on the dithiolate ligand as de-

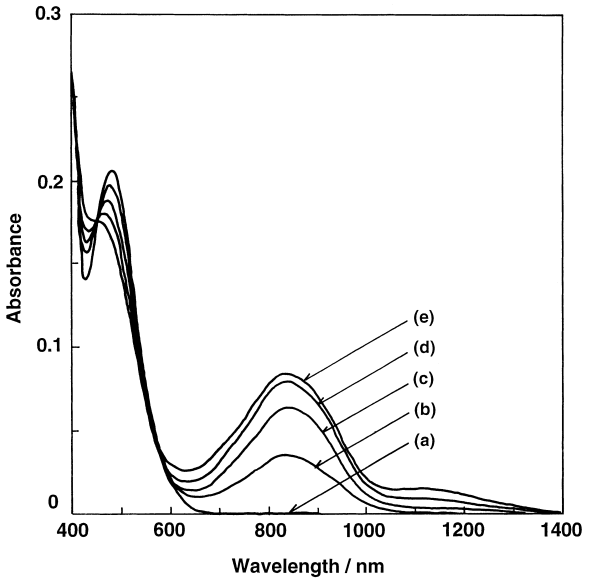

Fig. 8. Electronic absorption spectra of $[NBu^n_4]_2[Sn(C_8H_4S_8)_3]$ (**3**) (4.0×10^{-5} mol dm^{-3}) in DMF in the presence of iodine: a) 0, b) 1.5×10^{-5}, c) 2.1×10^{-5}, d) 3.1×10^{-5}, e) 4.1×10^{-5} mol dm^{-3}.

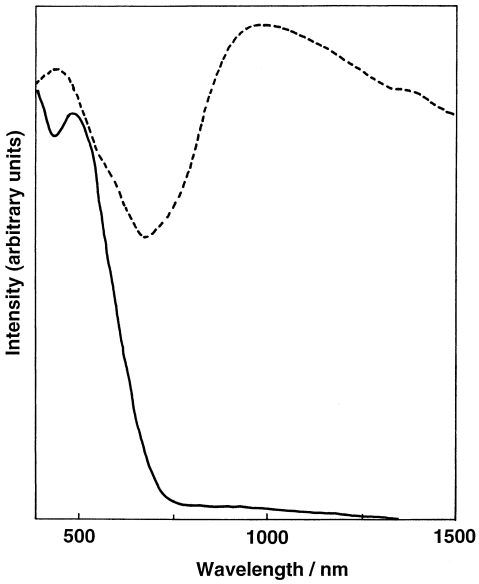

Fig. 9. Powder reflectance spectra of $[NBu^n_4]_2[Sn(C_8H_4S_8)_3]$ (**3**) (————) and $[Sn(C_8H_4S_8)_3]$ (**6**) (– – – – –).

scribed below. Similar CT bands were observed at longer wavelengths for the oxidized species of $[Ru(bpy)_2(C_8H_4S_8)]$ (bpy = 2,2′-bipyridine),[28] $[Co(\eta^5\text{-}C_5H_5)(C_8H_4S_8)]$,[13] $[Ti(\eta^5\text{-}C_5H_5)_2(C_8H_4S_8)]$ and $[Ti(\eta^5\text{-}C_5H_5)(C_8H_4S_8)_2]^-$ complexes.[15] Oxidation of **3** by iodine and TCNQ has afforded stable solids of the formally two electron-oxidized species **6**, which is in contrast to the immediate Sn–S bond cleavage of **1** and **2** upon oxidation. This may be due to more stabilization of the oxidized $C_8H_4S_8$ ligand compared with the C_3S_5 ligand. The oxidized complex **6** has exhibited an almost isotropic, broad ESR signal at $g = 2.008$ (peak-to-peak linewidth, 6.4 mT), which is due to the radical anion species contaminated in the essentially two-electron oxidized complex. This signal suggests the $C_8H_4S_8$ ligand-centered oxidation, as observed for other oxidized $C_8H_4S_8$-metal complexes.[7,12–16] A powder reflectance spectrum of **6** is shown in Fig. 9, together with that of **3**. Besides the band around 900 nm due to the oxidized species **6** (at 850 nm in DMF solution) ascribed to the metal-to-dithiolate ligand CT transition, bands are observed at longer wavelengths, which are due to molecular interactions through nonbonded S···S contacts in the solid state. Complex **6** has exhibited an electrical conductivitiy of 0.032 S cm^{-1} measured for a compacted pellet at room temperature. A molecular interaction among the oxidized $C_8H_4S_8$ moieties of **6** through S···S contacts described above forms an electron-conduction pathway in the solid state. Although many planar $C_8H_4S_8$ metal complexes were reported to be good electrical conductors,[6,7] it is noteworthy that the present bulky, hexa-coordinate metal complex exhibits a high electrical conductivity, as reported for some hexa-coordinate $[M(C_3S_5)_3]^{n-}$ [M = Mo(IV), W(IV) and Re(V); $n < 1$][9,10] and $[Co(\eta^5\text{-}C_5H_5)(C_8H_4S_8)]^+$ [13] and $[Ti(\eta^5\text{-}C_5H_5)(C_8H_4S_8)_2]^{0.3+}$ complexes.[15]

The oxidation of **4** or **5** by TCNQ in THF or DMF has afforded insoluble solids of **7** having the composition of $(C_8H_4S_8)_n$, which seem to come from the combination of $C_8H_4S_8$ moieties formed by the Sn–S bond cleavage, as observed for **9** formed by the oxidation of **1** or **2**. Solids of **7** also have shown an essentially isotropic ESR signal at $g = 2.008$, which indicates the presence of a small amount of an organic radical species. **7** has exhibited an electrical conductivity of 7.5×10^{-4} S cm^{-1} measured for a compacted pellet at room temperature. This comes from the molecular interactions through S···S contacts in the solid state, as observed for the above-mentioned crystal structure of $(C_3S_5)_2$. Powders of **6** have been further reacted with excess iodine to afford black solids of $[(C_8H_4S_8)(I_{0.9})]_n$. They contain the I_3^- and I_5^- ions as a counter ion, which have been confirmed by the stretching bands of these anions observed at 109 and 157 cm^{-1} in the Raman spectrum.[44,45] They have shown an isotropic, broad ESR signal at $g = 2.007$. The electrical conductivity is greatly increased (0.15 S cm^{-1} measured for a compacted pellet at room temperature) compared with that of **7**, which is due to an effective carrier-doping by iodine in the molecular system constructed with accelerated S···S contacts among the further oxidized $C_8H_4S_8$ moieties.

We are grateful to Professor S. Suzuki (Graduate School of Science, Osaka University) for the measurement of ESR spectra and to Dr. I. Kawafune (Osaka Municipal Technical Institute) for the measurement of X-ray photoelectron spectra. This research was supported in part by Grants-in-Aid for Scientific Research (Nos. 12023225 and 13029071) from the Ministry of Education, Science, Sports and Culture and by a Strategic Research Base Upbringing Special Coordination Fund for Promoting Science and Technology.

References

1 P. Cassoux, L.Valade, K. Kobayashi, A. Kobayashi, R. A. Clark, and A. E. Underhill, *Coord. Chem. Rev.*, **110**, 115 (1991).

2 G. Matsubayashi, "Reviews on Heteroatom Chemistry," Myu, Tokyo (1991), Vol. 4, p.171.
3 R.-M. Olk, B. Olk, W. Dietzsch, R. Kirmse, and E. Hoyer, *Coord. Chem. Rev.*, **117**, 99 (1992).
4 A. E. Pullen and R.-M. Olk, *Coord. Chem. Rev.*, **188**, 211 (1999).
5 M. Nakano, A. Kuroda, T. Maikawa, and G. Matsubayashi, *Mol. Cryst. Liq. Cryst.*, **284**, 301 (1996).
6 M. Nakano, A. Kuroda, and G. Matsubayashi, *Inorg. Chim. Acta*, **254**, 189 (1997).
7 M. Nakano, A. Kuroda, H. Tamura, R. Arakawa, and G. Matsubayashi, *Inorg. Chim. Acta*, **279**, 165 (1998).
8 G. Matsubayashi, M. Nakano, and H. Tamura, *Coord. Chem. Rev.*, **226**, 143 (2002).
9 G. Matsubayashi, K. Douki, H. Tamura, M. Nakano, and W. Mori, *Inorg. Chem.*, **32**, 5990 (1993).
10 G. Matsubayashi, T. Maikawa, and M. Nakano, *J. Chem. Soc., Dalton Trans.*, **1993**, 2995.
11 G. Matsubayashi, T. Maikawa, H. Tamura, M. Nakano, and R. Arakawa, *J. Chem. Soc., Dalton Trans.*, **1996**, 1539.
12 G. Matsubayashi, M. Nakano, K. Saito, T. Yonamine, and R. Arakawa, *J. Organomet. Chem.*, **611**, 364 (2000).
13 H. Mori, M. Nakano, H. Tamura, and G. Matsubayashi, *J. Organomet. Chem.*, **574**, 77 (1999).
14 G. Matsubayashi, M. Nakano, K. Saito, and H. Tamura, *Mol. Cryst. Liq. Cryst.*, **343**, 29 (2000).
15 K. Saito, M. Nakano, H. Tamura, and G. Matsubayashi, *Inorg. Chem.*, **39**, 4815 (2000).
16 K. Saito, M. Nakano, H. Tamura, and G. Matsubayashi, *J. Organomet. Chem.*, **625**, 7 (2001).
17 S. M. S. V. Doidge-Harrison, R. A. Howie, J. T. S. Irvine, G. Spencer, and J. L. Wardell, *J. Organomet. Chem.*, **414**, C5 (1991).
18 S. M. S. V. Doidge-Harrison, R. A. Howie, J. T. S. Irvine, G. M. Spencer, and J. L. Wardell, *J. Organomet. Chem.*, **436**, 23 (1992).
19 S. M. S. V. Doidge-Harrison, R. A. Howie, J. T. S. Irvine, and J. L. Wardell, *Polyhedron*, **17**, 2223 (1992).
20 S. M. S. V. Doidge-Harrison, J. T. S. Irvine, A. Khan, G. M. Spencer, J. L. Wardell, and J. H. Aupers, *J. Organomet. Chem.*, **516**, 199 (1996).
21 H. Buchanan, R. A. Howie, A. Khan, G. M. Spencer, J. L. Wardell, and J. H. Aupers, *J. Chem. Soc., Dalton Trans.*, **1996**, 541.
22 A. Khan, J. N. Low, J. L. Wardell, and G. Ferguson, *Acta Crystallogr. Sect. C*, **54**, 1399 (1998).
23 Z. H. Cholan, R. A. Howie, and J. L. Wardell, *J. Organomet. Chem.*, **577**, 140 (1999).
24 G. Steimecke, H. J. Seitler, R. Kirmse, and E. Hoyer, *Phosphorus Sulfur*, **7**, 49 (1979).
25 L. Valade, J.-P. Lrgros, M. Bousseau, P. Cassoux, M. Barbauskas, and L. Interrante, *J. Chem. Soc., Dalton Trans.*, **1985**, 783.
26 N. Svenstrup, K. M. Rasmussen, T. K. Kansen, and J. Becher, *Synthesis*, **1994**, 809.
27 L. Binet, J. M. Fabre, C. Montginoul, K. B. Simonsen, and J. Becher, *J. Chem. Soc., Perkin Trans., 1*, **1996**, 783.
28 K. Natsuaki, M. Nakano, and G. Matsubayashi, *Inorg. Chim. Acta*, **299**, 112 (2000).
29 A. Nakahama, M. Nakano, and G. Matsubayashi, *Inorg. Chim. Acta*, **284**, 55 (1999).
30 T. Higashi, "ABSCOR: Program for absorption correction," Rigaku Corporation, Tokyo (1995).
31 A. C. T. North, D. C. Philips, and F. C. Mathews, *Acta Crystallogr. Sect. A*, **24**, 351 (1968).
32 G. M. Sheldrick, "SHELX 86: Program for the solution of crystal structure," University of Göttingen, Germany (1985).
33 A. Altomare, G. Cascarano, C. Giacovazzo, A. Guagliardi, M. C. Burla, G. Polidori, and M. Camalli, *J. Appl. Crystallogr.*, **27**, 435 (1994).
34 G. M. Sheldrick, "SHELXL: Program of the refinement of crystal structure," University of Göttingen (1997).
35 "teXsan: Crystal structure Analysis Package," Molecular Structure Corp., The Woodlands, TX, 1992.
36 "International Tables for X-Ray Crystallography," Kynoch Press, Birmingham, England (1974), Vol. 4.
37 C. K. Johnson, "ORTEP-II, Report ORNL-5138," Oak Ridge National Laboratory, Oak Ridge, TN (1976).
38 G. Matsubayashi, K. Takahashi, and T. Tanaka, *J. Chem. Soc., Dalton Trans.*, **1988**, 967.
39 X. Yang, T. B. Rauchfuss, and S. Wilson, *J. Chem. Soc., Chem. Commun.*, **1990**, 34.
40 X. Yang, T. B. Rauchfuss, and S. Wilson, *J. Am. Chem. Soc.*, **111**, 3465 (1989).
41 F. Matsuda, H. Tamura, and G. Matsubayashi, *Inorg. Chim. Acta*, **295**, 243 (1999).
42 G. Matsubayashi, T. Ryowa, H. Tamura, M. Nakano, and R. Arakawa, *J. Organomet. Chem.*, **645**, 94 (2002).
43 N. Svenstrup and J. Becher, *Synthesis*, **1995**, 215.
44 M. Cowie, A. Gleizes, G. W. Grynkewich, D. W. Kalina, M. S. McClure, R. P. Scaringe, R. C. Teitelbaum, S. L. Ruby, J. A. Ibers, C. R. Kannewurf, and T. J. Marks, *J. Am. Chem. Soc.*, **101**, 2921 (1979).
45 B. N. Diel, T. Inabe, J. W. Lyding, K. F. Schoch, Jr., C. R. Kannewurf, and T. J. Marks, *J. Am. Chem. Soc.*, **105**, 1551 (1983).